A THEORETICAL ANALYSIS OF THE FLUTTER OF ORTHOTROPIC PANELS EXPOSED TO A HIGH SUPERSONIC STREAM OF ARBITRARY DIRECTION

by Peter A. Gaspers, Jr., and Bass Redd

Ames Research Center

Moffett Field, Calif.

NASA TN D-3551

A THEORETICAL ANALYSIS OF THE FLUTTER OF ORTHOTROPIC

PANELS EXPOSED TO A HIGH SUPERSONIC STREAM

OF ARBITRARY DIRECTION

By Peter A. Gaspers, Jr., and Bass Redd

Ames Research Center
Moffett Field, Calif.

NATIONAL AERONAUTICS AND SPACE ADMINISTRATION

A THEORETICAL ANALYSIS OF THE FLUTTER OF ORTHOTROPIC

PANELS EXPOSED TO A HIGH SUPERSONIC STREAM

OF ARBITRARY DIRECTION

By Peter A. Gaspers, Jr., and Bass Redd
Ames Research Center

SUMMARY

A theoretical analysis of the flutter of flat, rectangular, orthotropic panels at various angles of orientation with respect to the flow direction is presented. The analysis is based on linear small deflection plate theory and static strip theory for aerodynamic forces. The partial differential equation of motion is then solved approximately, for panels with clamped or simply supported edges, using the Galerkin method.

Plots of the critical dynamic pressure parameter as a function of the number of Galerkin modes are presented to demonstrate convergence properties of Galerkin's method. It is shown that a large number of modes may be necessary to give converged solutions. Curves of the critical dynamic pressure parameter as a function of flow angle are presented for various combinations of stiffness ratios and length-to-width ratios.

INTRODUCTION

Exterior surface panels of supersonic aircraft and aerospace vehicles often must be capable of carrying not only air loads but also acoustic, vibration, and thermal loads. Skin structures which have demonstrated promising results are often orthotropic.

Past theoretical work on panel flutter has been devoted almost completely to rectangular isotropic panels having simply supported edge conditions with the air flow parallel to one edge. In some investigations (refs. 1, 2, and 3) orthotropic panels, clamped edge conditions, and arbitrary flow angles have been treated individually with no consideration being given to a combination of these parameters. In one previous investigation (ref. 4) simply supported orthotropic panels with arbitrary flow direction and midplane stresses were analyzed.

In this paper an analysis of a flat rectangular orthotropic panel clamped or simply supported on all four edges and exposed to a high supersonic flow of arbitrary direction is presented. The parameters used in the analysis are rigidity ratios, length-to-width ratio, flow angle, and the dynamic pressure parameter. The results are presented in a series of curves for various

combinations of the parameters, from which flutter boundaries can easily be calculated. Since modified linear piston theory is used for aerodynamic forces, the results are restricted to Mach numbers above approximately 1.6.

SYMBOLS

a	panel length
b	panel width
D_x	panel bending rigidity in x direction
D_y	panel bending rigidity in y direction
H	panel torsional rigidity
M	Mach number
$\overline{M}$	number of Galerkin modes in x direction
m,n,r,s	integers
$\overline{N}$	number of Galerkin modes in y direction
N_x,N_y	midplane stresses, positive in compression
N_{xy}	midplane shear stress
q	dynamic pressure
t	time
V	free-stream velocity
w	panel deflection
x,y,x_1,y_1	rectangular coordinates
α	eigenvalue
β	$\sqrt{M^2-1}$
γ	mass per unit area of panel
Λ	flow angle
λ	dynamic pressure parameter
λ_c	critical dynamic pressure parameter

ρ free-stream density

Φ differential operator defined in equation (2a)

THEORETICAL ANALYSIS

If linear small deflection plate theory and modified linear piston theory for aerodynamic loading are assumed, the partial differential equation of motion for a flat, rectangular, orthotropic plate with one side exposed to a high supersonic flow of arbitrary direction is:

$$D_x \frac{\partial^4 w}{\partial x^4} + 2H \frac{\partial^4 w}{\partial x^2 \partial y^2} + D_y \frac{\partial^4 w}{\partial y^4} + N_x \frac{\partial^2 w}{\partial x^2} + 2N_{xy} \frac{\partial^2 w}{\partial x \, \partial y} + N_y \frac{\partial^2 w}{\partial y^2}$$

$$+ \frac{2q}{\beta}\left(\frac{\partial w}{\partial x} \cos \Lambda + \frac{\partial w}{\partial y} \sin \Lambda + \frac{1}{V}\frac{\partial w}{\partial t}\right) + \gamma \frac{\partial^2 w}{\partial t^2} = 0 \qquad (1)$$

where $w = w(x,y,t)$ is the deflection and the coordinate system is shown in figure 1.

Making the transformation $x = ax_1$, $y = by_1$ and then dropping subscripts on x_1, y_1 for convenience, we can write equation (1) in the form:

$$\Phi w + \frac{\lambda a}{V}\frac{\partial w}{\partial t} + \frac{\gamma a^4}{D_x}\frac{\partial^2 w}{\partial t^2} = 0 \qquad (2)$$

where Φ is the differential operator

$$\Phi = \frac{\partial^4}{\partial x^4} + \frac{2Ha^2}{D_x b^2}\frac{\partial^4}{\partial x^2 \partial y^2} + \frac{D_y a^4}{D_x b^4}\frac{\partial^4}{\partial y^4} + R_x \frac{\partial^2}{\partial x^2} + \frac{2aR_{xy}}{b}\frac{\partial^2}{\partial x \, \partial y}$$

$$+ \frac{a^2 R_y}{b^2}\frac{\partial^2}{\partial y^2} + \lambda\left(\cos \Lambda \frac{\partial}{\partial x} + \frac{a}{b}\sin \Lambda \frac{\partial}{\partial y}\right) \qquad (2a)$$

and

$$R_x = \frac{N_x a^2}{D_x} \qquad R_{xy} = \frac{N_{xy} a^2}{D_x} \qquad R_y = \frac{N_y a^2}{D_x} \qquad \lambda = \frac{2qa^3}{\beta D_x}$$

Here x and y are dimensionless with a range from 0 to 1.

We assume a solution of equation (2) of the form:

$$w(x,y,t) = U(x,y)g(t) = Ug$$

Substitution in equation (2) gives

$$\Phi(Ug) + \frac{\lambda a}{V} \frac{\partial(Ug)}{\partial t} + \frac{\gamma a^4}{D_x} \frac{\partial^2(Ug)}{\partial t^2} = g\Phi U + \frac{\lambda a}{V} U\dot{g} + \frac{\gamma a^4}{D_x} U\ddot{g} = 0$$

or

$$\frac{\Phi U}{U} = -\frac{\lambda a}{V} \frac{\dot{g}}{g} - \frac{\gamma a^4}{D_x} \frac{\ddot{g}}{g} \tag{3}$$

Since the left side of this equation involves only x and y and the right side only t, both are equal to a constant which we call α and we have

$$\Phi U = \alpha U \tag{4}$$

$$\frac{\gamma a^4}{D_x} \ddot{g} + \frac{\lambda a}{V} \dot{g} = -\alpha g \tag{5}$$

Equation (4) together with the boundary conditions on U is an eigenvalue problem which can be solved approximately by the Galerkin method in which a linear combination of linearly independent functions, each of which satisfies the boundary conditions, is substituted for U.

We consider panels with clamped edges and panels with simply supported edges. For a panel with clamped edges the boundary conditions are

$$\left. \begin{array}{l} U(0,y) = U(1,y) = U(x,0) = U(x,1) = 0 \\[2mm] \dfrac{\partial U}{\partial x}(0,y) = \dfrac{\partial U}{\partial x}(1,y) = \dfrac{\partial U}{\partial y}(x,0) = \dfrac{\partial U}{\partial y}(x,1) = 0 \end{array} \right\} \tag{6}$$

A set of functions which satisfy these boundary conditions is

$$U_{mn}(x,y) = \psi_m(x)\psi_n(y)$$

The form for $\psi_m(x)$ is:

$$\psi_m(x) = \cos K_m x - \cosh K_m x + C_m(\sin K_m x - \sinh K_m x)$$

where

$$C_m = \frac{\cosh K_m - \cos K_m}{\sin K_m - \sinh K_m}$$

and where the K_m satisfy $\cosh K_m \cos K_m = 1$; the form for $\psi_n(y)$ is the same as that for $\psi_m(x)$.

For simply supported edges the boundary conditions are

$$U(0,y) = U(1,y) = U(x,0) = U(x,1) = 0$$

$$\frac{\partial^2 U}{\partial x^2}(0,y) = \frac{\partial^2 U}{\partial x^2}(1,y) = \frac{\partial^2 U}{\partial y^2}(x,0) = \frac{\partial^2 U}{\partial y^2}(x,1) = 0$$

A set of functions which satisfies these boundary conditions is

$$U_{mn}(x,y) = \sin m\pi x \sin n\pi y$$

Substituting

$$U = \sum_{n=1}^{\overline{N}} \sum_{m=1}^{\overline{M}} C_{mn} U_{mn}$$

in equation (4) gives:

$$\Phi\left(\sum_{n=1}^{\overline{N}} \sum_{m=1}^{\overline{M}} C_{mn} U_{mn}\right) - \alpha \sum_{n=1}^{\overline{N}} \sum_{m=1}^{\overline{M}} C_{mn} U_{mn} = 0 \tag{7}$$

or

$$\sum_{n=1}^{\overline{N}} \sum_{m=1}^{\overline{M}} C_{mn}(\Phi U_{mn} - \alpha U_{mn}) = 0 \tag{8}$$

Multiplying by U_{rs} and integrating over the panel we have:

$$\sum_{n=1}^{\overline{N}} \sum_{m=1}^{\overline{M}} C_{mn}\left(\int_0^1\int_0^1 U_{rs}\Phi U_{mn}\ dx\ dy - \alpha \int_0^1\int_0^1 U_{rs}U_{mn}\ dx\ dy\right) = 0$$

or

$$\sum_{n=1}^{\overline{N}} \sum_{m=1}^{\overline{M}} C_{mn}\left(L_{mnrs} - \alpha\delta_{mr}\delta_{ns}\right) = 0 \tag{9}$$

$$r = 1, 2, \ldots, \overline{M}$$

$$s = 1, 2, \ldots, \overline{N}$$

5

where

$$L_{mnrs} = \int_0^1 \int_0^1 U_{rs}\Phi U_{mn} \; dx \; dy$$

$$\delta_{mn} = \begin{cases} 1 & \text{if} \quad m = n \\ 0 & \text{if} \quad m \neq n \end{cases}$$

These integrals are straightforward for either the clamped or simply supported case and may be found in reference 5. The resulting formulas for L_{mnrs} are as follows:

For the clamped case:

$$L_{mnrs} = A_{mn}\delta_{mr}\delta_{ns} + \frac{2Ha^2}{D_x b^2} D_{rm}D_{sn} + \delta_{ns}(H_{rm}\lambda \cos \Lambda + D_{rm}R_x)$$

$$+ \; \delta_{mr}\left(\frac{a}{b} H_{sn}\lambda \sin \Lambda + \frac{a^2}{b^2} D_{sn}R_y\right) + 2 \frac{a}{b} R_{xy}H_{rm}H_{sn}$$

where

$$A_{mn} = K_m^4 + \frac{D_y a^4}{D_x b^4} K_n^4$$

$$D_{rm} = \frac{4K_r^2 K_m^2}{K_m^4 - K_r^4}(K_r C_r - K_m C_m)\left[(-1)^{m+r} + 1\right] \quad (m \neq r)$$

$$D_{mm} = -K_m C_m(K_m C_m + 2)$$

$$H_{rm} = \frac{4K_r^2 K_m^2}{K_m^4 - K_r^4}\left[(-1)^{r+m} - 1\right] \qquad (m \neq r)$$

$$H_{mn} = 0$$

For the simply supported case:

$$L_{mnrs} = \frac{1}{4} \delta_{mr}\delta_{ns}\left(m^4\pi^4 + 2m^2 n^2\pi^4 \frac{a^2 H}{b^2 D_x} + n^4\pi^4 \frac{a^4 D_y}{b^4 D_x} - m^2\pi^2 R_x - n^2\pi^2 \frac{a^2}{b^2} R_y\right)$$

$$+ \; \frac{2a}{b} R_{xy}P_{mr}P_{ns} + \frac{1}{2}\lambda \cos \Lambda\delta_{ns}P_{mr} + \frac{a}{2b}\lambda \sin \Lambda\delta_{mr}P_{ns}$$

6

where

$$P_{mn} = \left[(-1)^{m+n} - 1 \right] \frac{mn}{m^2 - n^2}$$

Equations (9) are linear and can be written in matrix form:

$$(A - \alpha I)C = 0 \tag{10}$$

$$A = (a_{ij}) \qquad a_{ij} = L_{mnrs}$$

$$i = (r - 1)\overline{N} + s \qquad j = (m - 1)\overline{N} + n$$

and I is the identity matrix.

The problem becomes that of finding the eigenvalues of the matrix A. In what follows we set $\lambda a/V$, in equation (5), to zero since for high supersonic speeds it has a negligible effect on the characteristic roots of equation (5). In this case when all eigenvalues are real, the motion is stable. If at least one pair of eigenvalues is a complex conjugate pair, the motion is unstable, that is, the amplitude increases with time. The value of $\lambda = 2qa^3/\beta D_x$ at which a conjugate pair of eigenvalues first appear is called the critical value and denoted λ_c. For values of λ above λ_c, flutter occurs.

The eigenvalues of the matrix A were computed with the IBM 7094 using an existing eigenvalue program. The values of λ_c were obtained by a trial and error converging process. The problem was programed for any n × n matrix from 4 × 4 to 100 × 100, where $n = \overline{MN}$, the product of the number of modes in the x direction and the y direction. The input could be any combination of the panel parameters and any number of eigenvalues could be computed. With $\overline{M} = 4$ and $\overline{N} = 6$, for example, the matrix A is 24 × 24 and consequently has 24 eigenvalues.

RESULTS AND DISCUSSION

The results of this analysis are presented in the form of plots of the critical dynamic pressure parameter, λ_c, as a function of the number of modes used and as a function of the flow angle Λ for various combinations of the stiffness ratios H/D_x and D_y/D_x and the length-to-width ratio a/b. The plots of λ_c versus the number of modes demonstrate the convergence proper- ties of Galerkin's method and the plots of λ_c versus Λ are flutter bound- aries for which a sufficient number of modes have been used to obtain a reasonably converged solution. Since we have used modified linear piston theory for aerodynamic loading, the results are restricted to Mach numbers above $M \simeq 1.6$. In this Mach number range the omission of the unsteady term in the aerodynamic loading can be shown to have only a small effect on the flutter boundaries. This is due to the imaginary part of the eigenvalue increasing quite rapidly above the flutter boundary and dominating the damp- ing contribution of the unsteady aerodynamic term. (Also see ref. 6.)

7

The problem of the convergence of Galerkin's method for this particular boundary value problem has not, so far as we know, been investigated. In the absence of proofs relating to convergence properties we have used the criterion that the solution is converging when it displays asymptotic behavior as a function of the number of modes; that is, when the difference between solutions with n modes and with $n + 1$ modes decreases as n increases we say that the solution is converging. For the cases where we have exact solutions it appears that the Galerkin method converges to the correct value.

Figure 1 shows the panel geometry. The supersonic flow of velocity V makes an angle Λ with the side of the panel at $y = 0$. The orthotropic axes of the plate are parallel to the sides, and D_X, the rigidity in the x direction, is always taken larger than D_Y in all of the calculations.

Figures 2(a) through 2(i) demonstrate convergence properties of Galerkin's method in the form of plots of λ_c versus the number of modes in the y direction for various values of a/b, H/D_X, D_y/D_X, Λ, and $\overline{M}$, where $\overline{M}$ is the number of modes in the x direction. Figures 2(a) and 2(b) for simply supported isotropic panels show that as the length-to-width ratio in the direction of the flow increases the number of modes required (to obtain convergence) increases very rapidly. At $a/b = 0.5$, 4 modes give a reasonably converged solution while at $a/b = 0.1$, 25 modes are required to give a solution within 10 percent of the exact value which was obtained by the method of reference 6.

Figures 2(c) and 2(d) are for a clamped isotropic panel with $\Lambda = 90^O$ using one mode in the x direction. The spanwise (x direction) modes are coupled for the clamped case but for $\Lambda = 90^O$ the inclusion of more spanwise modes makes only a small difference. The convergence is slightly slower but qualitatively very much the same as for the simply supported case. Hence, the clamped cases which correspond to converged simply supported cases are probably converged.

Figure 2(e) shows convergence properties for small flow angles of an isotropic panel with $a/b = 0.5$. For two modes in each direction ($\overline{M} = \overline{N} = 2$) the lower curves are obtained and show two stable regions. When $\overline{M} = \overline{N} = 4$, there are still two stable regions but when $\overline{M} = 4$ and $\overline{N} = 10$, the upper stable region vanishes while the main boundary remains unchanged. The upper stable regions for both $\overline{M} = \overline{N} = 2$ and $\overline{M} = \overline{N} = 4$ are thus seen to be spurious and due to unconverged solutions.

Figure 2(f) for an a/b of 0.1 shows two stable regions when $\overline{M} = \overline{N} = 4$, but the upper region vanishes when $\overline{N}$ is increased to 10. The curve for $\overline{M} = 4$ and $\overline{N} = 10$ represents a converged solution and for quite small flow angles is seen to depart substantially from the $\overline{M} = \overline{N} = 4$ boundary.

Figures 2(g) and 2(h) demonstrate the influence of orthotropy on convergence for square panels. In general, for fixed $D_y/D_X < 1$ and $a/b = 1$, the number of modes in the y direction required for convergence increases with the flow angle and with H/D_X. For values of Λ other than 90° at least two modes are required in the x direction, and near 0°; three or four modes may

be required, the particular value depending on the rigidity ratios. The convergence problem is most severe for very small D_y/D_x together with large H/D_x.

In figure 2(i) we have plotted λ_c versus $\overline{N}$ for a simply supported panel of $a/b = 1.0$, $D_y/D_x = 0.0002$, and $\Lambda = 90^\circ$ for $H/D_x = 0.15$ and $H/D_x = 0.5$. This case was analyzed by Bohon (ref. 4) using only 2 modes in each direction. It is evident from the figure that the solutions are not approaching convergence even with 50 modes. For the simply supported panel with $\Lambda = 90^\circ$ an exact solution can be obtained by the method of reference 6. The exact solution for $H/D_x = 0.15$ is $\lambda_c = 198$, and for $H/D_x = 0.5$ is 1197.3. For the 2-mode solution of reference 4 and for figure 2(i), $\lambda_c = 16.5$. The 2-mode solution is thus inaccurate by a factor of about 12 or, in other words, is about 8.5 percent of the correct value. For flow angles other than 90° or 0° no exact solutions have been obtained and the modal approach must be used. For the cases being considered (fig. 2(i)) a large number of modes in the y direction would be required even for flow angles as small as 5° and at least two modes would be required in the x direction. The maximum matrix size $\overline{MN} \times \overline{MN}$ of this analysis was limited to about 60×60 because of inherent limitations in the eigenvalue program.

Figures 3 through 5 are converged flutter boundaries for various combinations of the parameters. For values of λ_c in the region above a curve flutter occurs; for values below the curve the panel is stable. The criterion used for convergence was that λ_c should be at least 85 percent of the fully converged value. Since the fully converged value must be estimated by plotting λ_c as a function of the number of modes, the 85-percent criterion will be conservative in most cases. Figure 3 shows the variation of λ_c with flow angle for several values of a/b. Figure 4(a) shows the influence of flow angle on λ_c for three values of H/D_x with $D_y/D_x = 0.1$ and $a/b = 1$. The curve for $H/D_x = 1$ is curious in that it actually intersects the curves for smaller H/D_x and shows a minimum at about $\Lambda = 70^\circ$ rather than at 90°. This behavior is considered in more detail in the discussion of figure 5.

The significance of figure 4(a) is that the torsional rigidity H has little effect at flow angles near zero but very large influence near 90°. The influence of torsional rigidity is even more pronounced in the curves of figure 4(b) for $D_y/D_x = 0.01$. For $H/D_x = 0.01$, λ_c decreases very rapidly with increasing Λ. For higher values of H/D_x, the influence of flow angle is progressively less. The curves for $H/D_x = 1$ and $H/D_x = 0.5$ do not extend to $\Lambda = 90^\circ$ because convergence could not be obtained at the larger flow angles. Figure 5 shows λ_c as a function of H/D_x for a square panel with $D_y/D_x = 0.1$ at several small flow angles. For flow angles up to about 20°, the maximum λ_c actually occurs for H/D_x less than 1. At $\Lambda = 0^\circ$ the maximum λ_c occurs at $H/D_x \cong 0.5$. One would expect the maximum λ_c to occur at the maximum H/D_x but this is not the case for these flow angles. Figure 5 displays more clearly the behavior for small flow angles in figure 4(a).

It should be noted that the range of values of D_y/D_x and H/D_x that might occur in practice has not been well established. Several types of panels including rib-stiffened and corrugation-stiffened panels have been analyzed by considering them to be orthotropic and calculating or measuring

their equivalent stiffnesses by assuming homogeneity. (See ref. 7 for example.) The panel parameters $D_y/D_x = 0.0002$, $H/D_x = 0.15$, $a/b = 1.0$ (fig. 10) correspond approximately to values measured and calculated in reference 7 for a corrugation-stiffened panel. They are also typical of some skin panels that are being used on certain aerospace vehicles. Since a corrugation-stiffened panel is not truly homogeneous but has a periodic structure, it may possibly not be accurate to treat it as homogeneous in a flutter analysis if a large number of modes are needed in the solution. As the modal wavelength approaches the structural cell size the theoretical model may not accurately represent the physical situation.

Finally, for reference, we have included the midplane stress terms, N_x, N_y, N_{xy}, in the equations but have made no calculations for nonzero stresses.

<div align="center">CONCLUSIONS</div>

For a fixed bending stiffness ratio D_y/D_x and length-to-width ratio, the critical dynamic pressure parameter λ_c, and hence the dynamic pressure at flutter, is strongly dependent on the torsional stiffness ratio H/D_x. In particular, for values of H/D_x near D_y/D_x, λ_c is very sensitive to a small change in flow angle, Λ, near $\Lambda = 0°$.

In theoretical work employing the Galerkin method, the accuracy of the results obtained must be considered carefully. We have shown that for isotropic panels with high length-to-width ratios and for most orthotropic panels including those of practical importance, a large number of Galerkin modes is required to obtain converged solutions.

Ames Research Center
    National Aeronautics and Space Administration
        Moffett Field, Calif., April 21, 1966

REFERENCES

1. Kordes, Eldon E.; and Noll, Richard B.: Theoretical Flutter Analysis of Flat Rectangular Panels in Uniform Coplanar Flow With Arbitrary Direction. NASA TN D-1156, 1962.

2. Nelson, Herbert C.; and Cunningham, Herbert J.: Theoretical Investigation of Flutter of Two-Dimensional Flat Panels With One Surface Exposed to Supersonic Potential Flow. NACA TN 3465, 1955.

3. Kordes, Eldon E.; Tuovila, Weimer J.; and Guy, Lawrence D.: Flutter Research on Skin Panels. NASA TN D-451, 1960.

4. Bohon, Herman L.: Flutter of Flat Rectangular Orthotropic Panels With Biaxial Loading and Arbitrary Flow Direction. NASA TN D-1949, 1963.

5. Felgar, Robert P., Jr.: Formulas for Integrals Containing Characteristic Functions of a Vibrating Beam. Circular no. 14, Bureau of Engineering Research, Univ. Texas, 1950.

6. Hedgepeth, John M.: Flutter of Rectangular Simply Supported Panels at High Supersonic Speeds. J. Aero. Sci., vol. 24, no. 8, Aug. 1957, pp. 563-573, 586.

7. Stroud, W. Jefferson: Elastic Constants for Bending and Twisting of Corrugation-Stiffened Panels. NASA TR R-166, 1963.

12
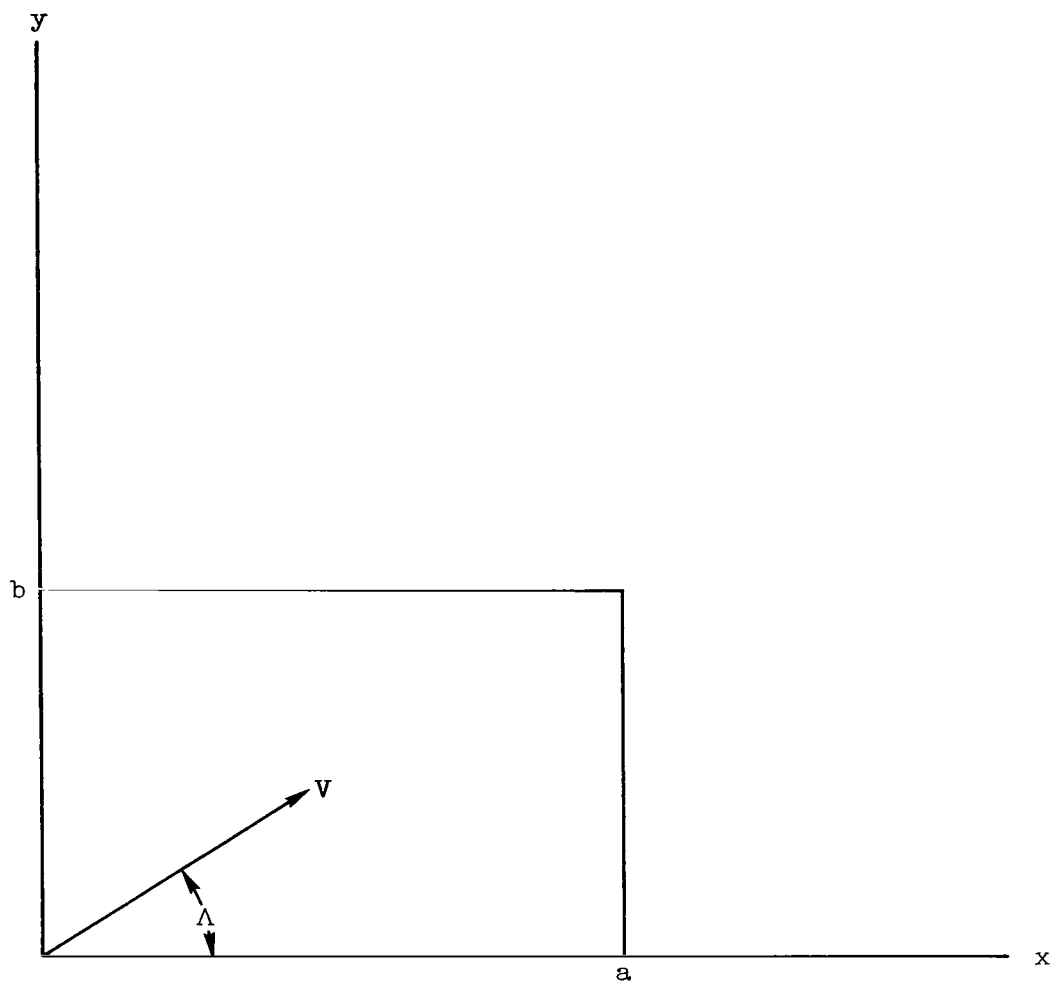
Figure 1.- Coordinate system and panel geometry.
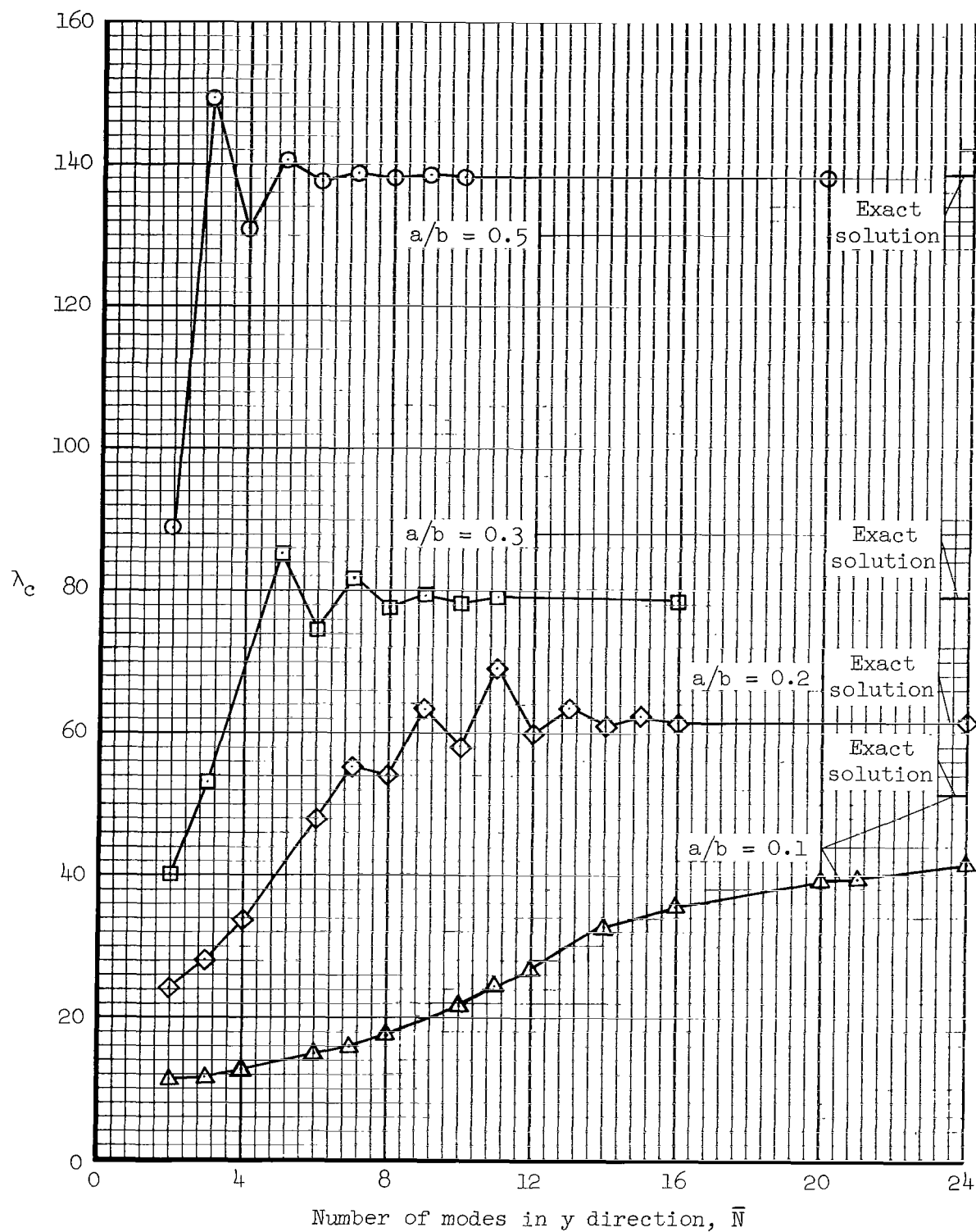
(a) Simply supported: $H/D_X = D_y/D_X = 1.0$; $\Lambda = 90^\circ$; $\overline{M} = 1$.

Figure 2.- Convergence of Galerkin's method.
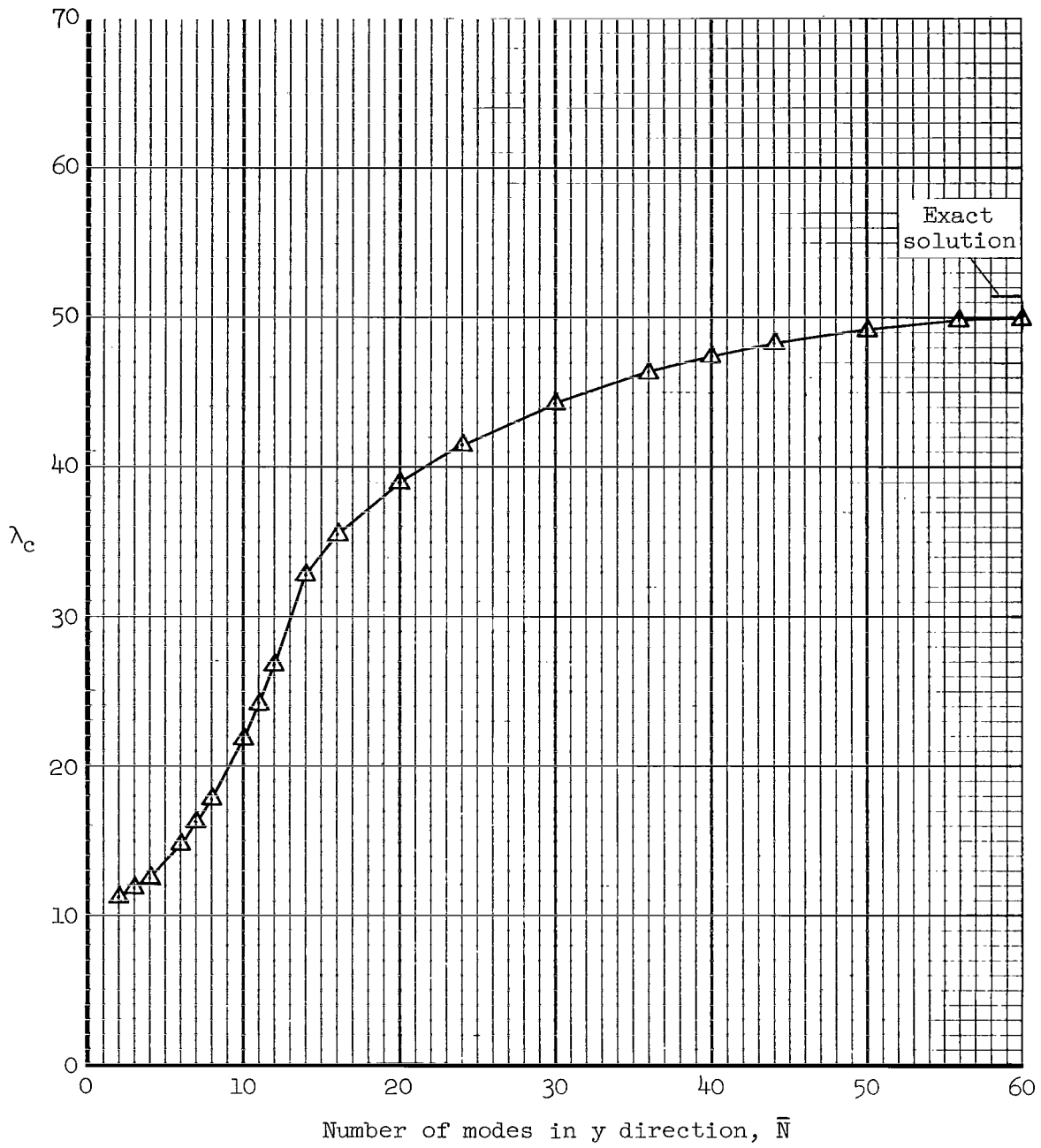
(b) Simply supported: $a/b = 0.1$; $H/D_x = D_y/D_x = 1.0$; $\Lambda = 90^\circ$; $\overline{M} = 1$.
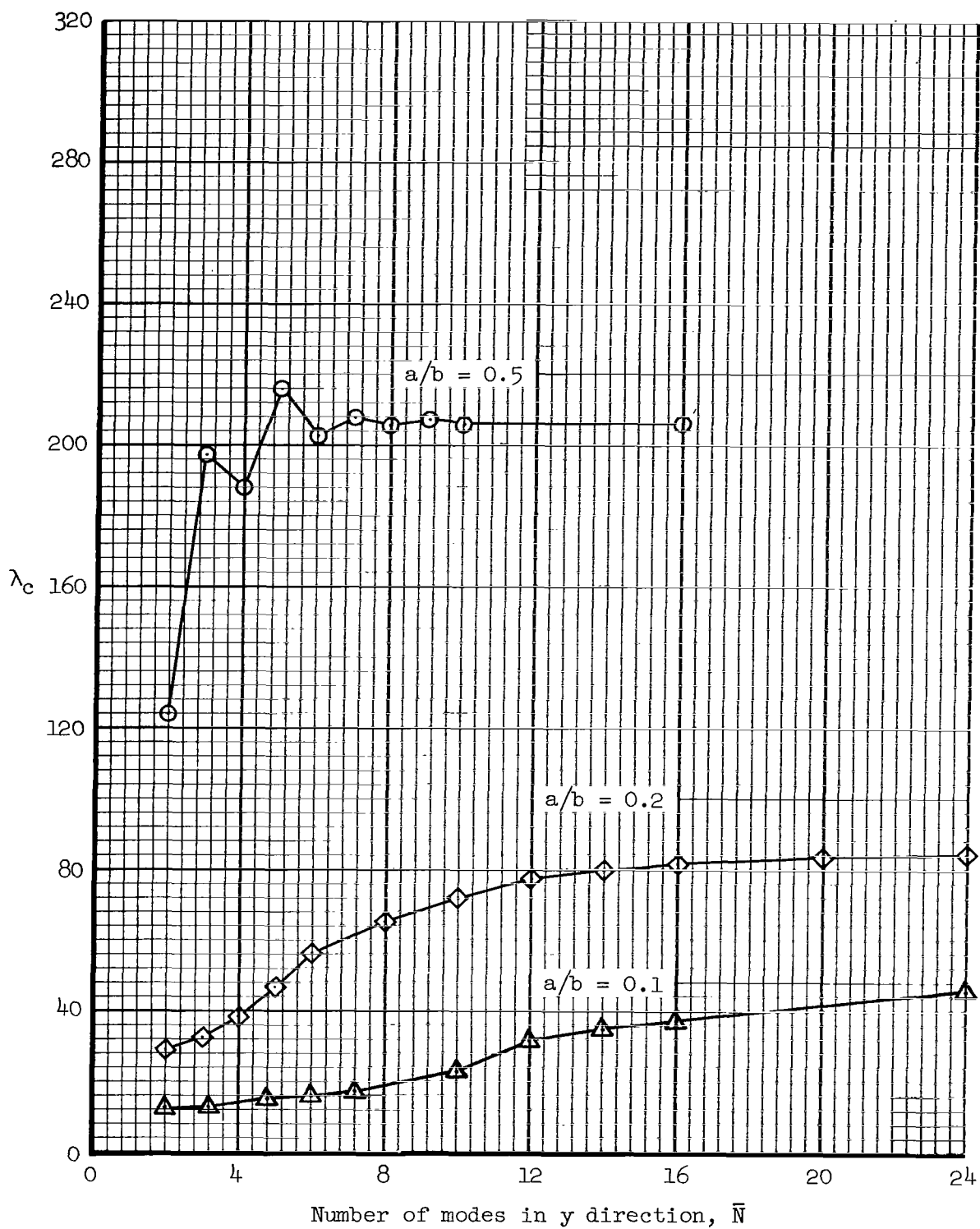
Figure 2.- Continued.

(c) Clamped: $H/D_x = D_y/D_x = 1.0$; $\Lambda = 90°$; $\overline{M} = 1$.
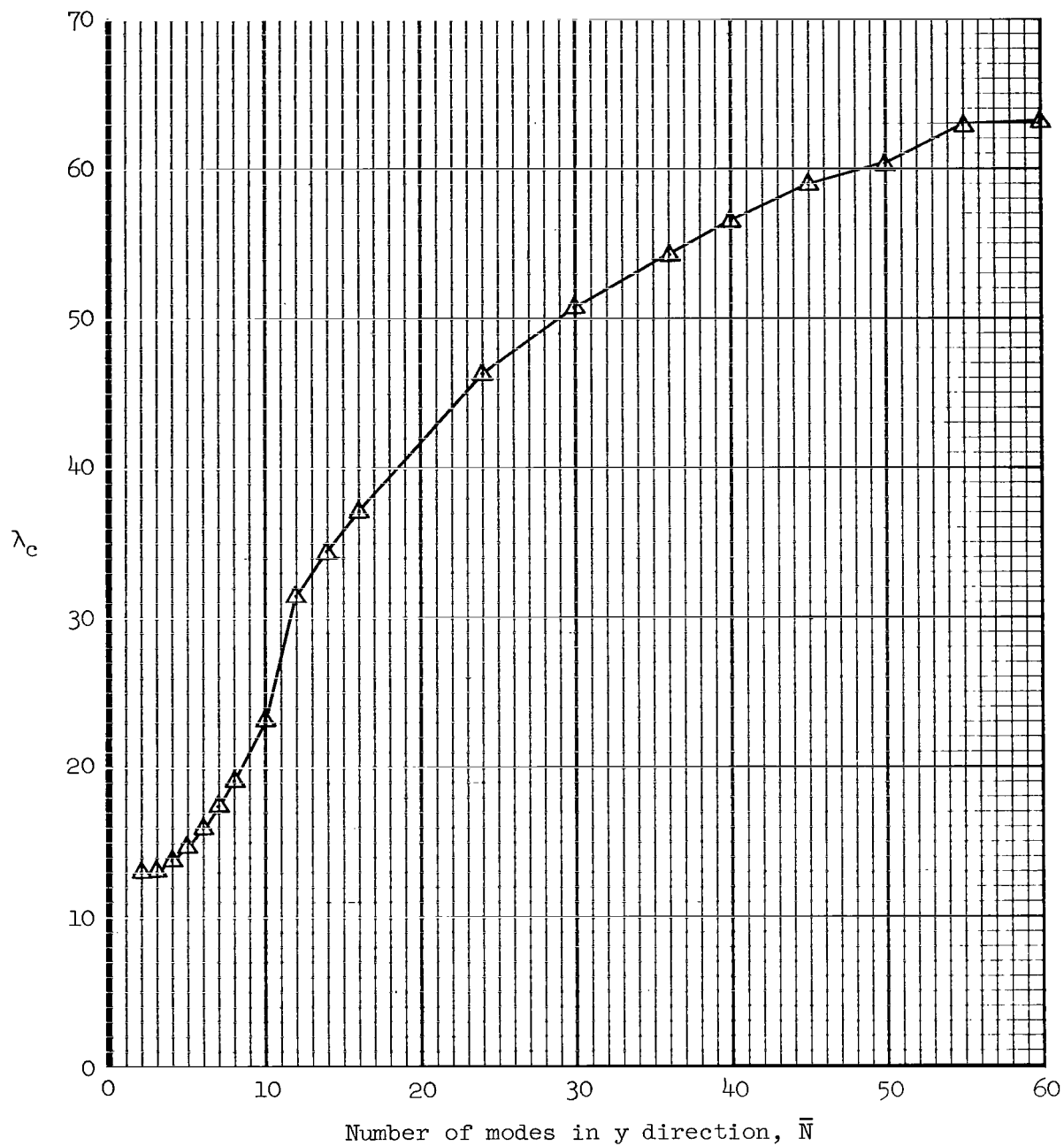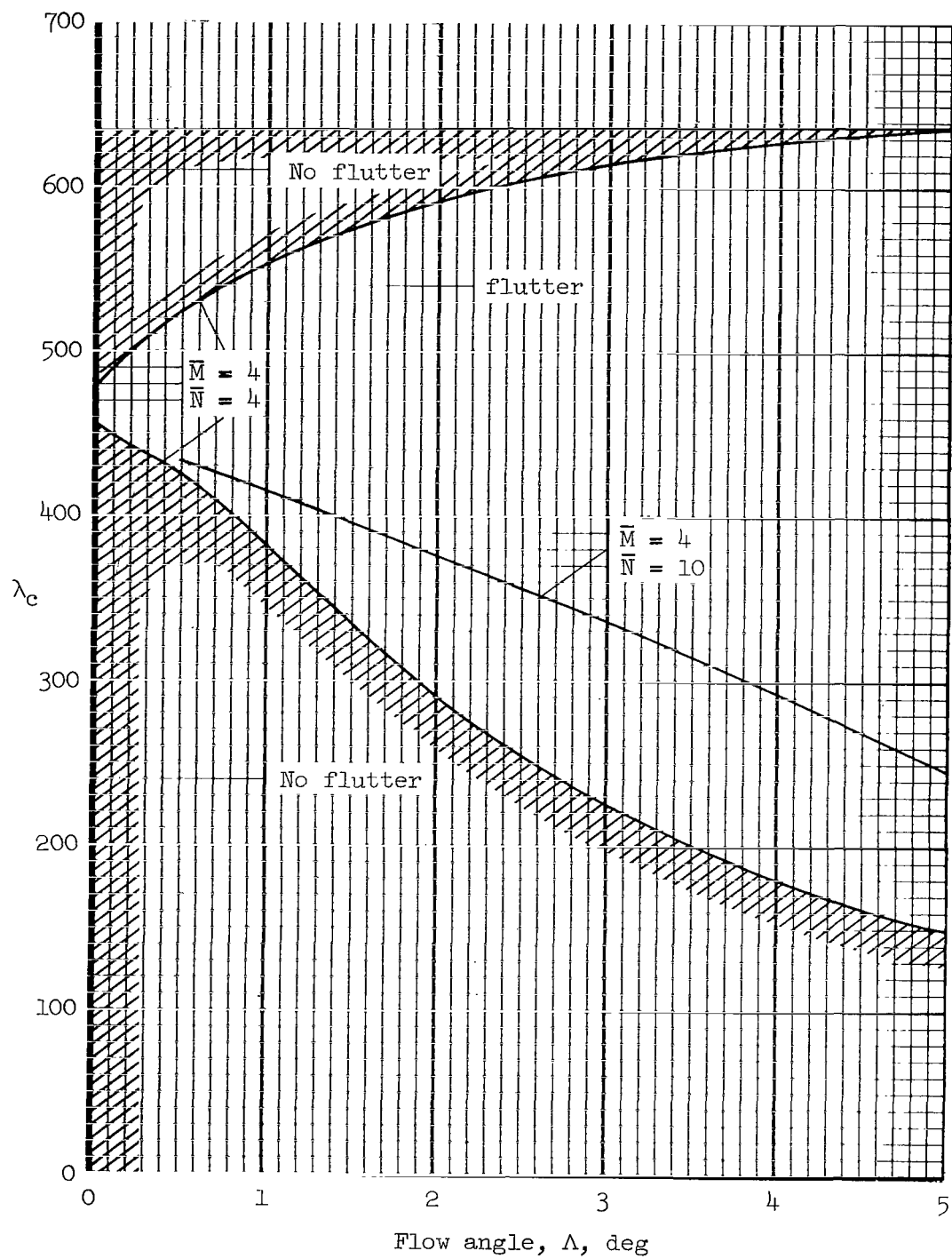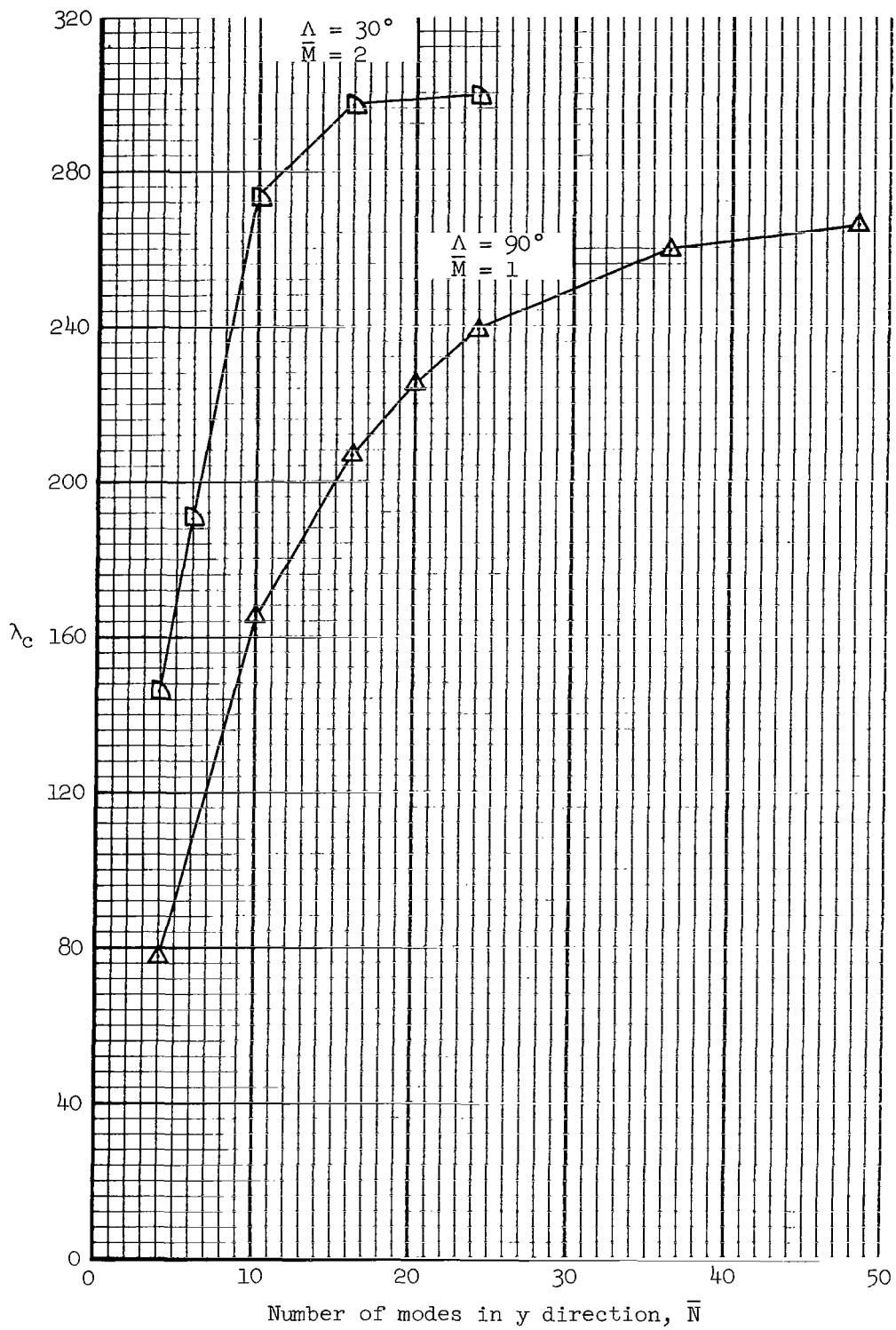
Figure 2.- Continued.

(d) Clamped: $a/b = 0.1$; $H/D_x = D_y/D_x = 1.0$; $\Lambda = 90^{\circ}$; $\overline{M} = 1$.
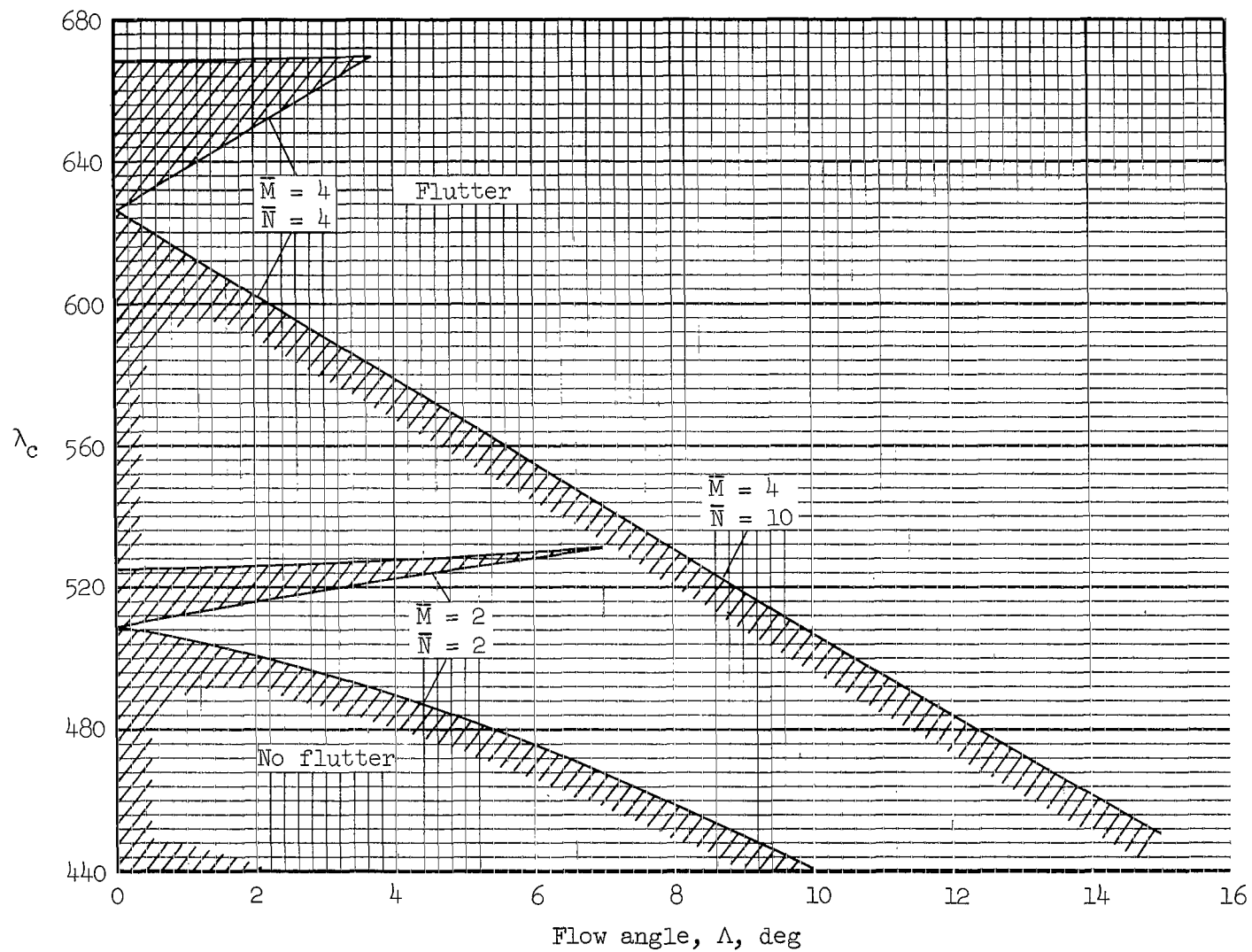
Figure 2.- Continued.

(e) Clamped: $a/b = 0.5$; $H/D_x = D_y/D_x = 1.0$.

Figure 2.- Continued.

(f) Clamped: a/b = 0.1; $H/D_x = D_y/D_x = 1.0$.

Figure 2.- Continued.

(g) Clamped: a/b = 1.0; D_y/D_x = 0.01; H/D_x = 0.5.

Figure 2.- Continued.
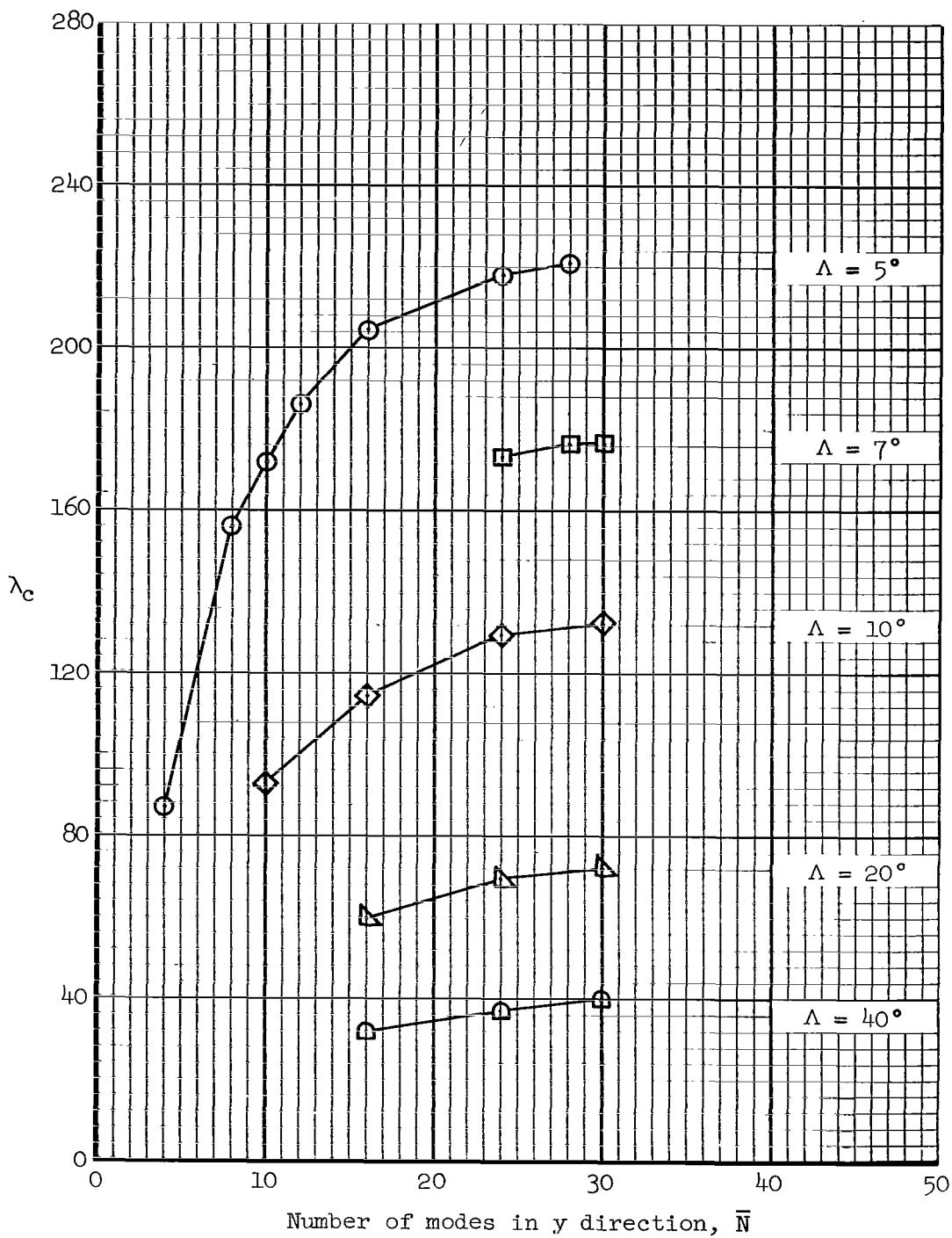
(h) Clamped: a/b = 1.0; H/D_x = 0.05; D_y/D_x = 0.001; $\overline{M}$ = 2.

Figure 2.- Continued.
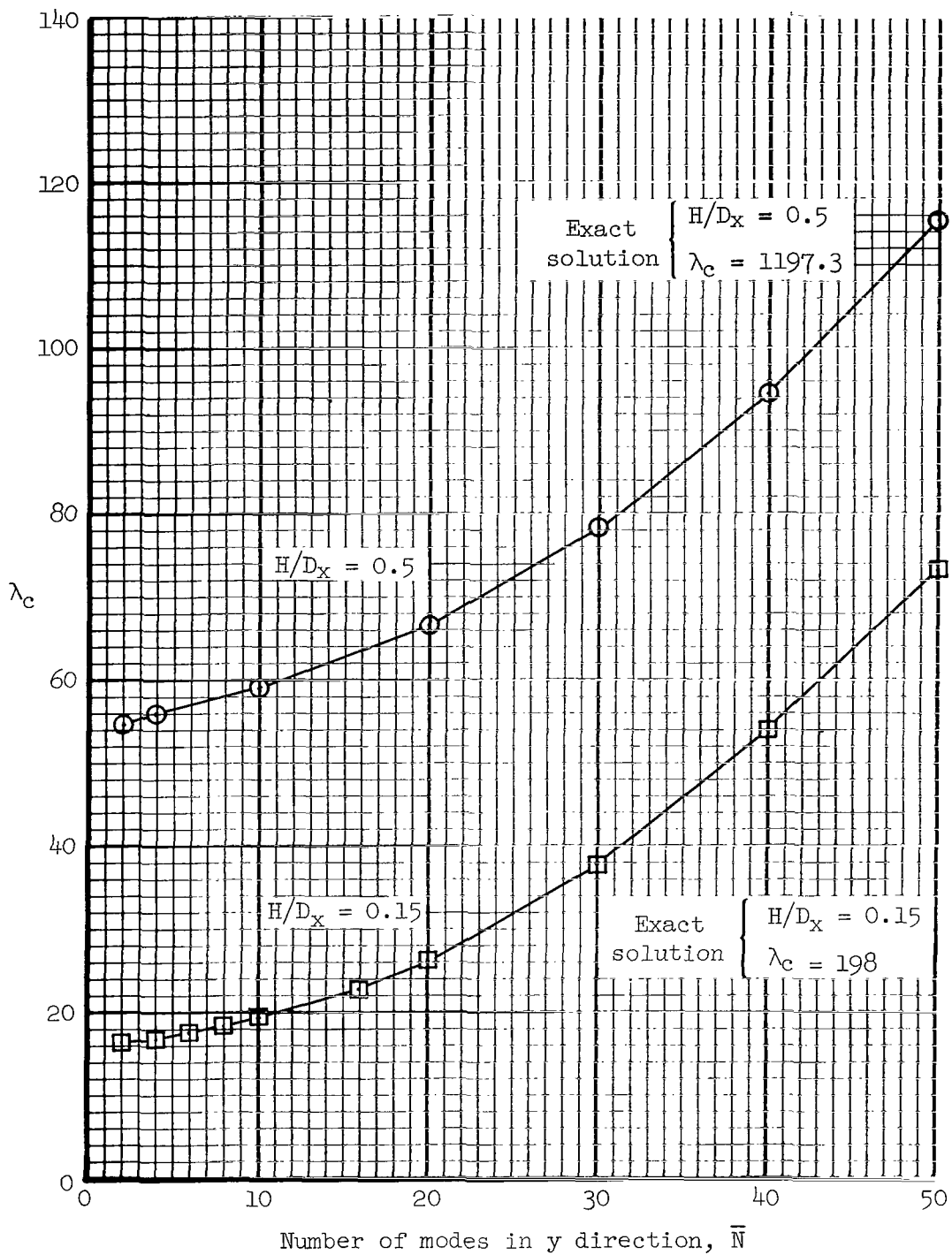
(i) Simply supported: $a/b = 1.0$; $D_y/D_x = 0.0002$; $\Lambda = 90^\circ$; $\overline{M} = 1$.
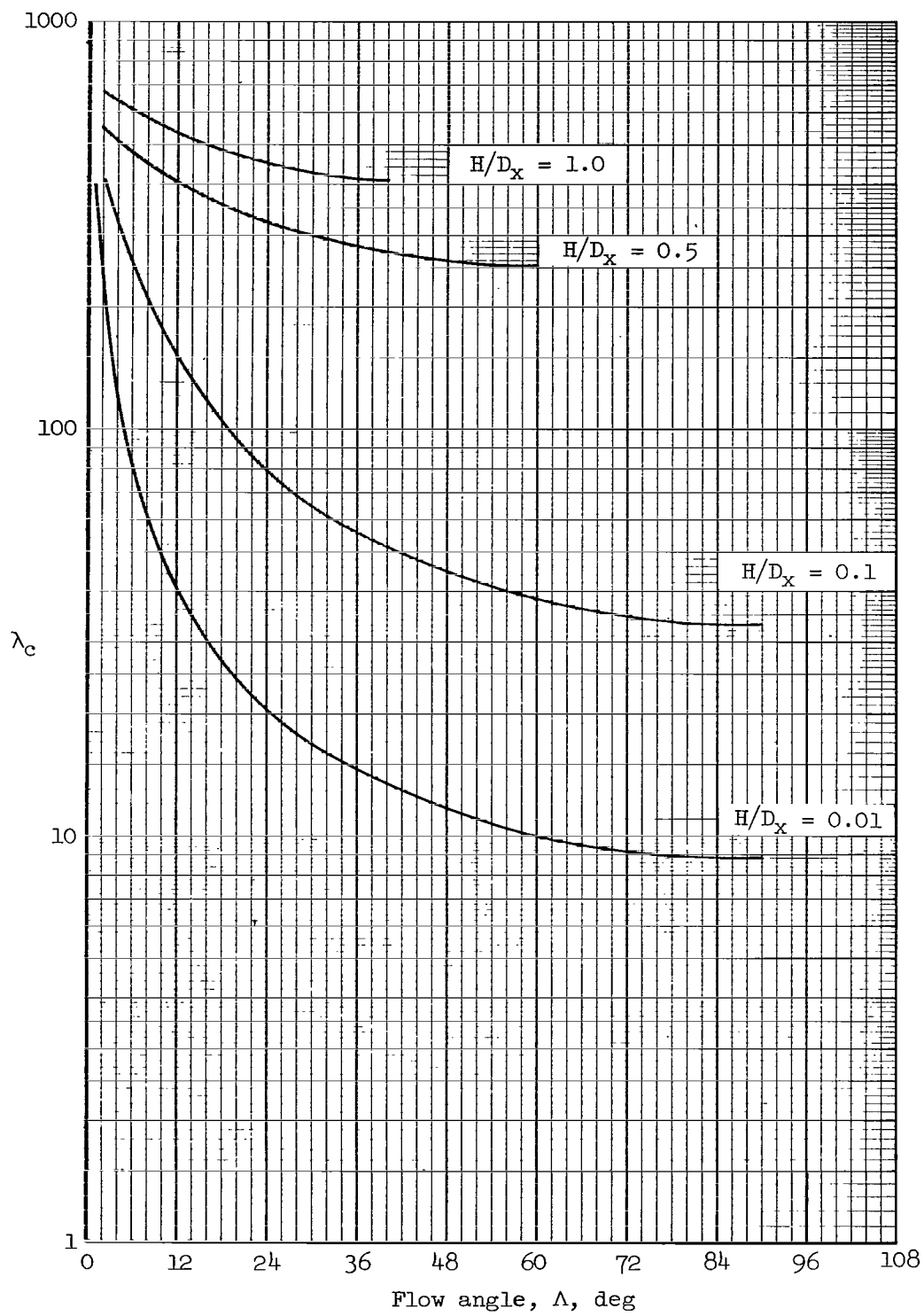
Figure 2.- Concluded.
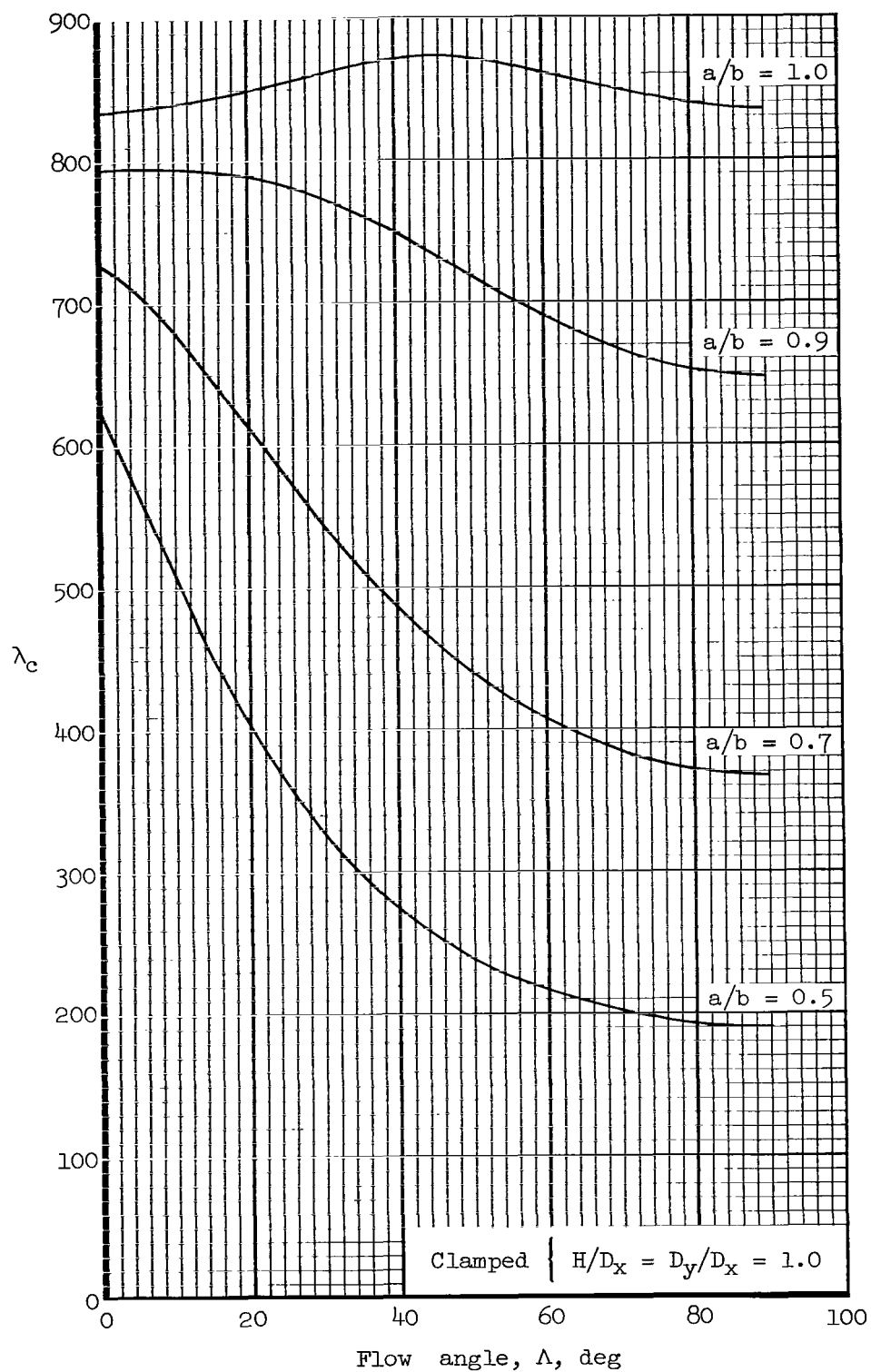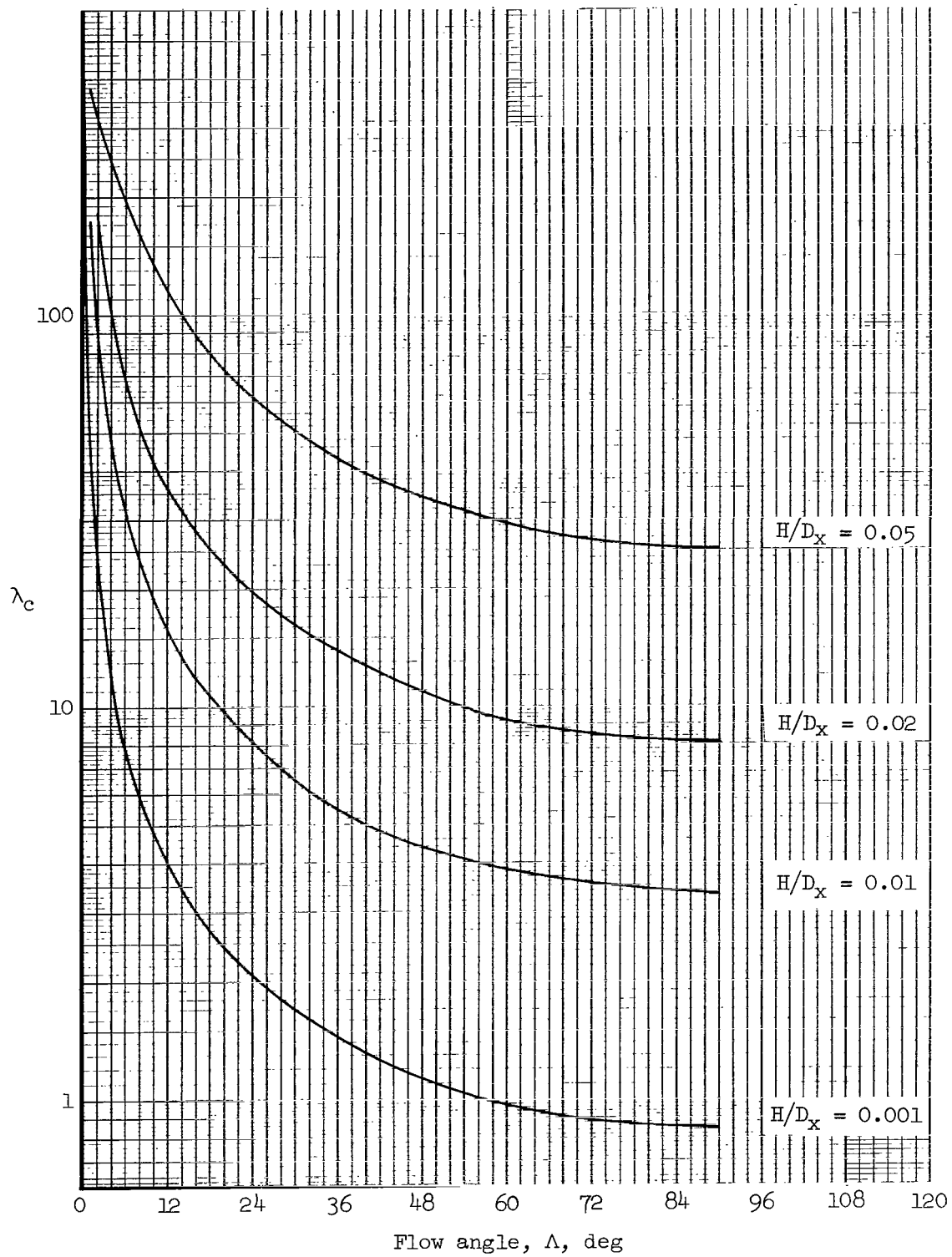
Figure 3.- Effect of flow angle and length-to-width ratio.
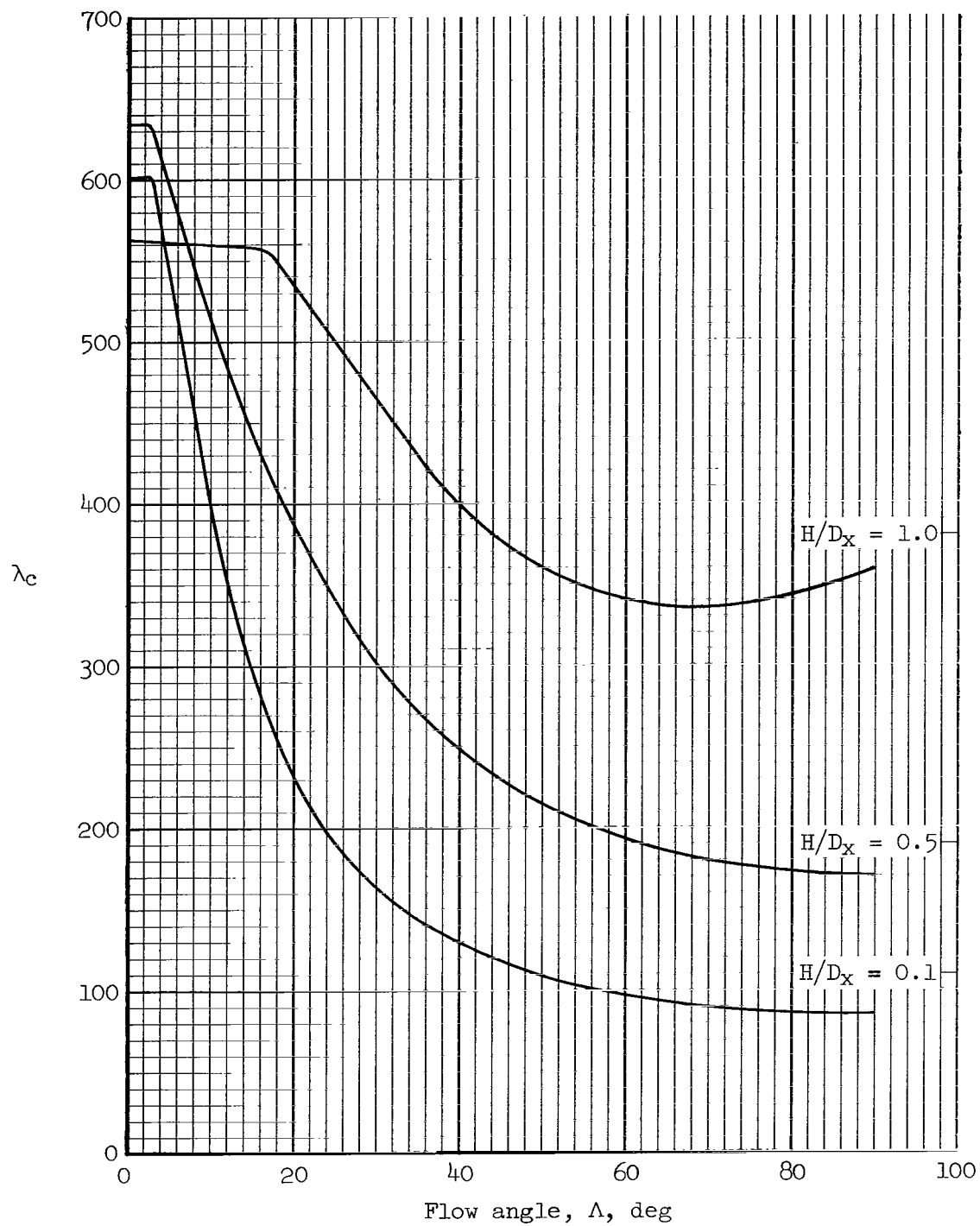
(a) Clamped: $a/b = 1.0$; $D_y/D_x = 0.1$; $\overline{M} = 4$; $\overline{N} = 10$.

Figure 4.- Effect of flow angle and rigidity ratio.

The vertical axis is labeled λ_c and ranges from 1 to 1000.
The horizontal axis is labeled "Flow angle, Λ, deg" ranging from 0 to 108.

Curves labeled:
$H/D_x = 1.0$
$H/D_x = 0.5$
$H/D_x = 0.1$
$H/D_x = 0.01$

(b) Clamped: $a/b = 1.0$; $D_y/D_x = 0.01$.

Figure 4.- Continued.

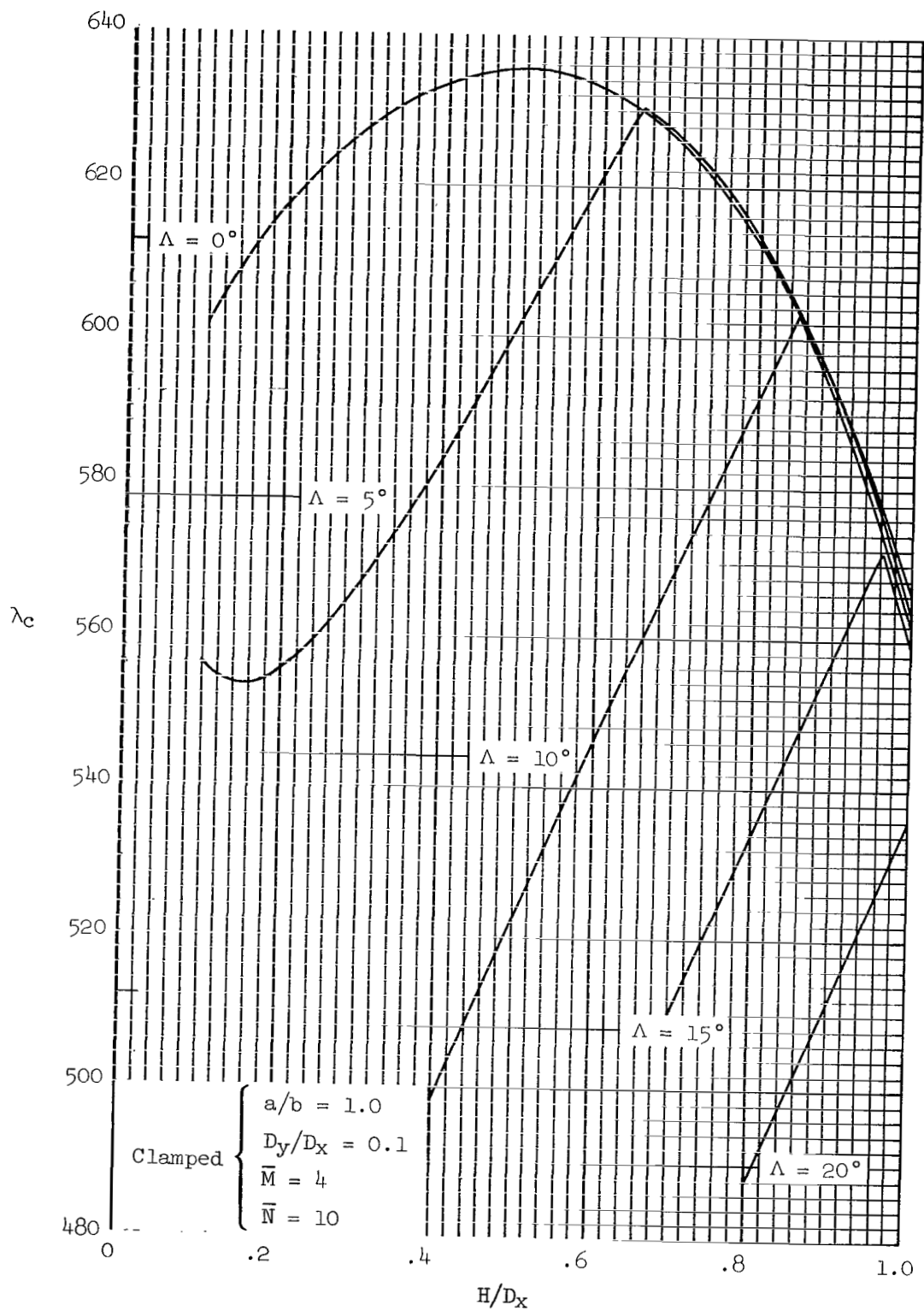(c) Clamped: $a/b = 1.0$; $D_y/D_x = 0.001$.

Figure 4.- Concluded.

Figure 5.- Effect of rigidity ratio and flow angle.

NASA SCIENTIFIC AND TECHNICAL PUBLICATIONS

TECHNICAL REPORTS: Scientific and technical information considered important, complete, and a lasting contribution to existing knowledge.

TECHNICAL NOTES: Information less broad in scope but nevertheless of importance as a contribution to existing knowledge.

TECHNICAL MEMORANDUMS: Information receiving limited distribution because of preliminary data, security classification, or other reasons.

CONTRACTOR REPORTS: Technical information generated in connection with a NASA contract or grant and released under NASA auspices.

TECHNICAL TRANSLATIONS: Information published in a foreign language considered to merit NASA distribution in English.

TECHNICAL REPRINTS: Information derived from NASA activities and initially published in the form of journal articles.

SPECIAL PUBLICATIONS: Information derived from or of value to NASA activities but not necessarily reporting the results of individual NASA-programmed scientific efforts. Publications include conference proceedings, monographs, data compilations, handbooks, sourcebooks, and special bibliographies.

Details on the availability of these publications may be obtained from:

SCIENTIFIC AND TECHNICAL INFORMATION DIVISION

NATIONAL AERONAUTICS AND SPACE ADMINISTRATION

Washington, D.C. 20546